Available online at www.sciencedirect.com
SCIENCE DIRECT®
Journal of Organometallic Chemistry 688 (2003) 192–199
Journal of Organometallic Chemistry
www.elsevier.com/locate/jorganchem

Spin–spin interaction between phenoxyl radicals through σ–π system

Toshiyuki Iida, Joji Ohshita *, Nobuaki Ohta, Kenji Komaguchi, Yoshiteru Itagaki, Masaru Shiotani, Atsutaka Kunai *

Department of Applied Chemistry, Graduate School of Engineering, Hiroshima University, Higashi-Hiroshima 739-8527, Japan

Received 24 June 2003; received in revised form 4 September 2003; accepted 4 September 2003

Abstract

Compounds having two *p*-phenoxyl radicals bridged by a 1,2-diphenylenedisilanylene unit in *m*,*p*- and *p*,*p*- fashions were synthesized and the intramolecular spin–spin interaction was examined by Curie plots of ESR signal intensities due to the $\Delta M_S = \pm 2$ transition at low temperature. It was found that bridging two phenoxyl radicals at meta and para positions of the bridge led to triplet ground state or degeneracy of triplet/singlet states. In contrast, two phenoxyl radicals put at both para positions interacted in an antiferromagnetic fashion through the diphenylenedisilanylene bridge, to realize singlet ground state.

Keywords: Spin state; Phenoxyl radical; σ–π Conjugation

1. Introduction

σ–π Conjugated organosilicon compounds are of great interest, regarding their potential utilities as novel functional materials [1]. For example, it has been demonstrated that polymers composed of a regularly alternating arrangement of an organosilicon unit and a π-system can be used as precursors of organic semiconductors, photo-conductors, and hole-transport materials.

On the other hand, several approaches have been examined to obtain organic high-spin molecules based on π-conjugated systems as spin couplers [2,3]. Recent example includes applications of phenylene [3b,c], thienylene [3d], pyridylene [3e], pyrrole-1,2,5-triyl [3f,g], triazine-2,4,6-triyl [3h], ethynylenephenylene [3i], phenylenevinylene [3j] and anthryleneethynylene [3k], to the high spin couplers.

However, only a little is known for σ–π systems as spin couplers. It has been demonstrated by Iwamura et al that bridging phenylnitrenes by a disilanylene unit at the meta and para positions gives rise to the successful high-spin coupling of the nitrenes [4].

Recently, we synthesized di- and monosilanylene bridged phenyl nitroxides (Chart 1, $n = 1, 2$) and found that they exhibit relatively large spin exchange integrals at 298 K and triplet state is involved in this systems by the ESR studies [5]. We also carried out ESR and SQUID measurements of the silanylene-bridged phenyl nitroxides ($n = 1–3$) at low temperature [6]. Interestingly, the disilanylene unit bridging the phenyl nitroxides at meta and para positions works as a ferromagnetic spin coupler, while bridging two phenyl nitroxides by a disilanylene unit at both para positions leads to an antiferromagnetic coupling. In contrast, mono- and trisilanylene bridges play only an ambiguous role in the spin-spin coupling. However, the nitroxide units may not retain the coplanarity with the adjacent phenylene group, which suppresses the delocalization of the radical center into the whole molecular system, in particular at low temperature. In this paper, we report the synthesis of silicon-bridged phenoxyl radicals, in which the radical centers are anticipated to be delocalized to the conjugated system than that in phenyl nitroxides. Their spin states were studied by temperature dependent ESR measurements.

* Corresponding authors. Tel.: +81-824-24-7727; fax: +81-824-22-5494.
E-mail addresses: jo@hiroshima-u.ac.jp (J. Ohshita), akunai@hiroshima-u.ac.jp (A. Kunai).

0022-328X/03/$ - see front matter © 2003 Elsevier B.V. All rights reserved.
doi:10.1016/j.jorganchem.2003.09.004

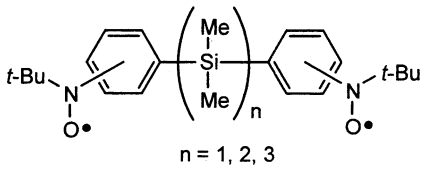

Chart 1.

2. Results and discussion

2.1. Preparation of mono- and disilanylene-bridged phenoxyl radicals

Precursors of phenoxyl radicals (**2a** and **2b**) were obtained as shown in Scheme 1. Thus, 3,5-di-*tert*-butyl-4-(trimethylsiloxy)phenyllithium reacted with 1,2-dichlorotetramethyldisilane or dichlorodimethylsilane to afford silicon-bridged silyl-protected phenol derivatives (**1a** and **1b**). Deprotection of the phenol unit by treating **1a** and **1b** with methyllithium then water gave precursors **2a** and **2b** [7]. However, attempted preparation of silanylene-bridged phenoxyl radicals **3a** and **3b** by oxidation of **2a** and **2b** with PbO_2 failed and no ESR active species were found to be formed in the mixtures. Even when the ESR measurements of the reaction mixtures were performed at low temperature, immediately after the interaction of **2a** and **2b** with PbO_2, no signals could be detected at all. The oxidation reactions always gave diphenoquinone as the sole isolable product, as shown in Scheme 1. Although the reaction mechanism is not clear yet, it seems likely that phenoxyl radicals **3a** and **3b** once formed undergo intramolecular coupling with loss of the silanylene moiety, which would be converted to unidentified silanols and siloxanes by interaction with excess PbO_2.

2.2. Preparation of diphenylenedisilanylene-bridged phenoxyl radicals

Next, we prepared 1,2-diphenylenedisilanylene-bridged phenoxyl radicals (**6pp** and **6mp**), as shown in Scheme 2. Thus, similar to the preparation of **2a** and **2b**, silyl-protected hydroxybiphenyl units were introduced to a disilane core to give **4pp** and **4mp**. Deprotection of the silyl capping groups by hydrolysis gave the expected precursors (**5pp** and **5mp**). When precursors **5pp** and **5mp** were treated with excess PbO_2 in 2-methylTHF (MTHF), the colorless solutions rapidly turned purple. The resulting mixtures were stirred vigorously until the O–H stretching absorptions disappeared in the IR spectra. Spin densities of the resulting samples were determined by ESR spectrometries to be 60 and 40% for **6pp** and **6mp**, respectively.

2.3. ESR spectra of phenoxyl radicals *6pp* and *6mp*

Phenoxyl radicals **6pp** and **6mp** thus prepared are labile to an extent and removal of the solvent gave ESR silent sticky liquid. They decomposed gradually even in solutions. In fact, standing the solution of **6pp** in MTHF at room temperature over night led to a decrease of the spin density to 27%.

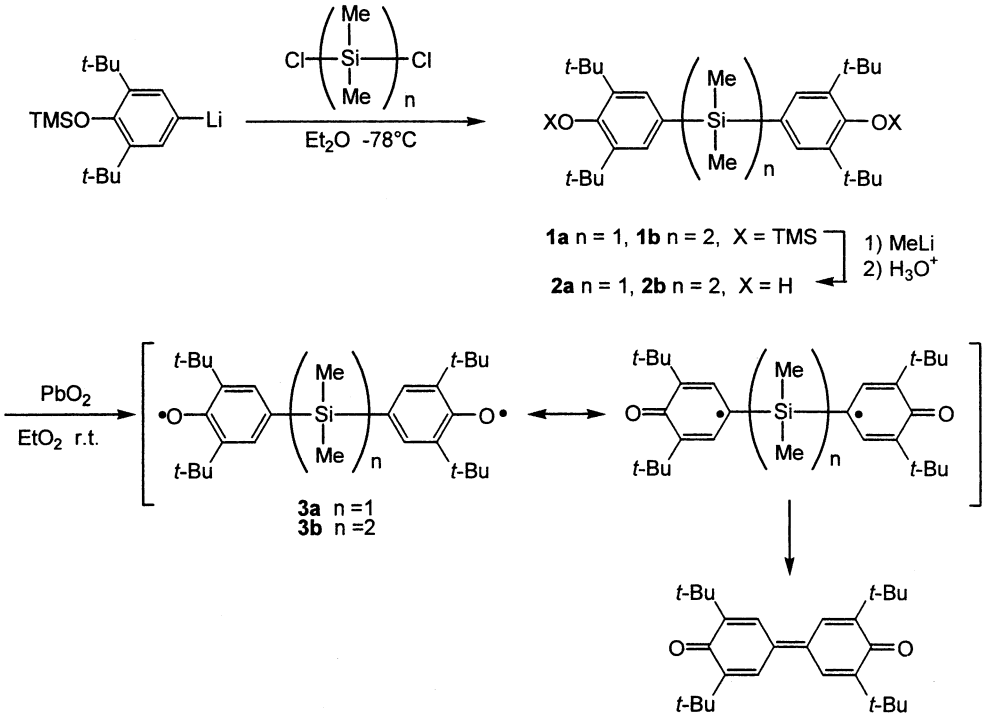

Scheme 1.

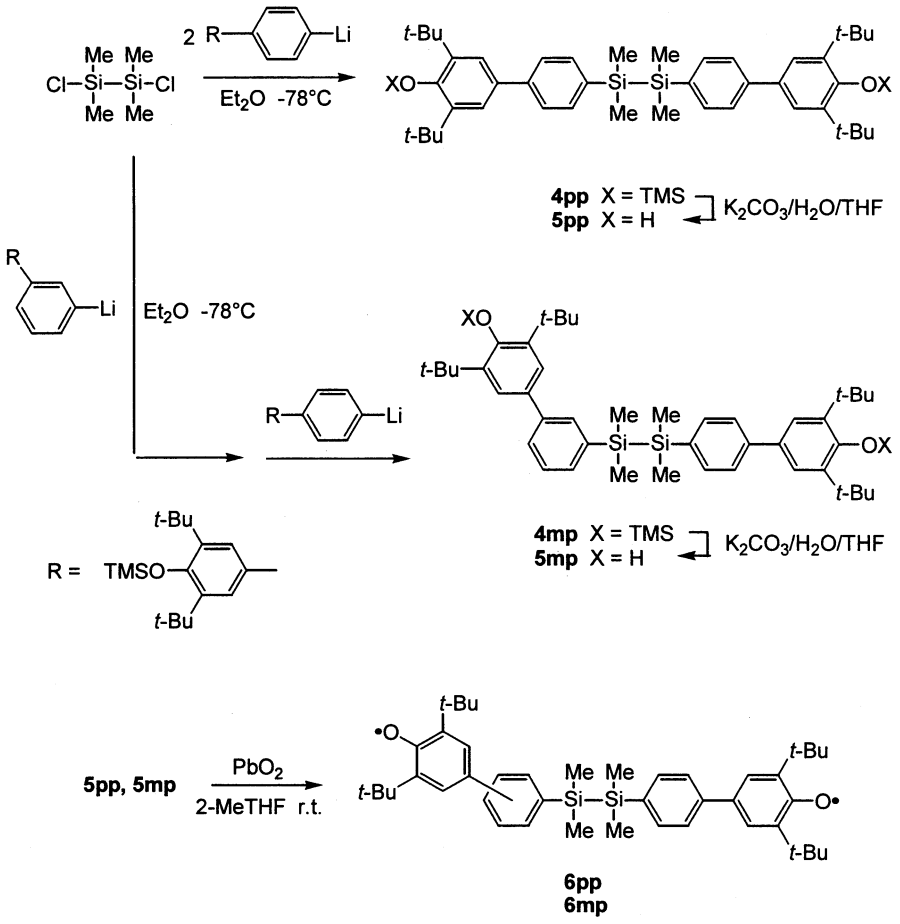

Scheme 2.

After filtration of Pb salts, the filtrates were subjected to the following ESR studies without purification. The ESR spectra of phenoxyl radicals **6pp** and **6mp** in MTHF showed a sharp singlet signal in the $\Delta M_S = \pm 1$ ($g \approx 2$) region at room temperature, which was a little broadened by lowering the temperature. At 77 K, a signal due to $\Delta M_S = \pm 2$ forbidden transition ascribed to triplet species was observed at $g \approx 4$, as shown in Fig. 1 for **6mp**. The signal of $\Delta M_S = \pm 2$ were doubly integrated to give Curie Plots (Fig. 2). As shown in Fig. 2, the plots for **6pp** deviated from linearity in the low temperature region, indicating that **6pp** has singlet ground state. In contrast, the signal intensity of **6mp** was proportional to the reciprocal of absolute temperature. This indicates that **6mp** has triplet ground state or singlet and triplet at degenerated states.

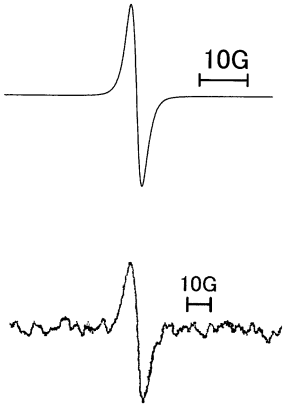

Fig. 1. ESR signals of **6mp** (a) due to the $\Delta M_S = \pm 1$ transition at room temperature, and (b) the $\Delta M_S = \pm 2$ transition at 77 K.

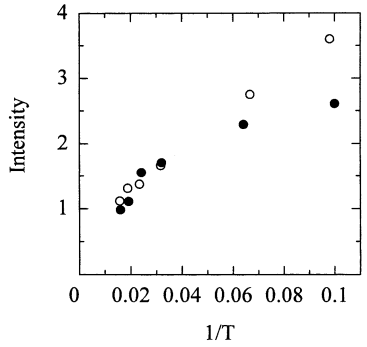

Fig. 2. Curie plots for the ESR signals at $\Delta M_S = \pm 2$ of (●) **6pp** and (○) **6mp**.

2.4. MO calculations

In order to ensure the spin state of compound **6mp**, we carried out ab initio MO calculations on model molecules (phenol **7mp** and diradical **8mp** in Chart 2), having hydrogens in place of *t*-butyl groups of **5mp** and **6mp**, respectively. Both the geometry optimization and the energy calculations for **7mp** were performed at the RB3LYP/6-31G level, while for **8mp**, the geometries were optimized on the triplet states at the level of UB3LYP/6-31G and the energy calculations of both singlet and triplet states were performed at the level of UB3LYP/6-31+G(d) on the optimized geometries. From the calculations, compound **8mp** was found to have triplet ground state with the singlet-triplet energy gap of 3.12 cal mol^{-1}, agreeing with the experimental results described above.

In addition, the spin densities of triplet states of **8mp** were calculated. In these calculations, both the geometry optimization and energy calculations were performed at the level of UB3LYP/6-31+G(d). The optimized geometry of **8mp** obtained from the calculations processes a little twisted biphenylene units with the torsion angles of 29.9 and 31.9° for *p*,*p*- and *m*,*p*-biphenylene units, respectively. The Si–Si bond is almost perpendicular with respect to the adjacent phenylene rings with the angles of 86.2 and 85.1°, respectively, to allow the σ–π type orbital interaction. Fig. 3 represents the Mulliken spin densities on the heavy atoms of **8mp**, derived from the calculations. As shown in Fig. 3, the aromatic carbons carry fairly high spin densities with the minimum absolute value of 0.032 for the Si-attached *m*-phenylene carbon, indicating the delocalization of the phenoxyl spins over the respective π-electron systems. It is also found that spins lie also on the two silicon atoms to an extent, although the Mulliken spin densities on the silicons are a little low. Interestingly, the spin–spin interaction in **8mp** is understood by using simple spin polarization up–down rule, that is, all spin signs in the molecule are alternately arranged, as is observed in ethenylene-bridged phenoxyl radicals [8].

When optimized structures of **7mp** and **8mp** are compared at the level of RB3LYP/6-31G and UB3LYP/6-31G, respectively, it is found that the O–C bond distances in **8mp** (1.28 and 1.29 Å) are much shorter than in **7mp** (1.39 Å), as expected. Bond distances in the phenylene rings of **7mp** range from 1.39 to 1.41 Å, indicating that no evident deformation is involved. In contrast, the phenoxyl units in **8mp** possess long C(O)–C(H) (1.44 Å) and C(C)–C(H) (1.42 Å) bonds, and short C(H)–C(H) (1.37 Å) bonds, in accordance with the spin delocalization. However, such deformation is not clear in the Si-attached inner phenylene rings, whose C–C bond distances are all in the range of 1.39–1.41 Å. The phenylene–phenylene bonds in **8mp** are a little shortened by about 0.1 Å, as compared with those in **7mp**.

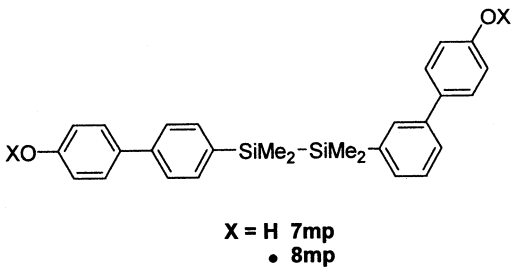

Chart 2.

2.5. Crystal structure of *2b*

The crystal structure of **2b** was determined by a single crystal X-ray diffraction study. The ORTEP drawing of **2b** is depicted in Fig. 4. All bond distances and angles are in the normal range. As can be seen in Fig. 4, the phenylene rings are located in an anti form with respect to the Si–Si bond (C1–Si1–Si1*–C1* = 180.0°). The angle between the Si–Si bond and the mean plane of the attached phenylene ring is 77.5°. These bonding features around the disilane unit almost retained in the optimized structure of **7mp**, in which Si–Si–C–C dihedral angles are about 85°. Other structural parameters of **2b** also closely resemble those of **7mp** derived from the calculations, indicative of the reliability of the MO calculations on **7mp**.

3. Conclusion

In conclusion, we demonstrated that the substitution mode of the phenylene units play a vital role on the spin–spin interaction through the σ–π systems. Although we could not carry out the SQUID measurements on **6pp** and **6mp**, due to their thermally unstable properties, it seems to be highly likely that the disilanylene bridge behaves as like an ethenylene linkage, which couples *p*- and *m*-phenoxyl radicals in a ferromagnetic fashion and *p*-, *p*- ones in an antiferromagnetic way [8]. The MO calculations also predicted that the disilanylene bridge may be able to couple spins, similar to ethenylene linkage.

4. Experimental

4.1. General

All reactions were carried out under an inert atmosphere. The work-up process mentioned below includes hydrolysis of the reaction mixture with aqueous ammonium chloride, separation of the organic layer, extrac-

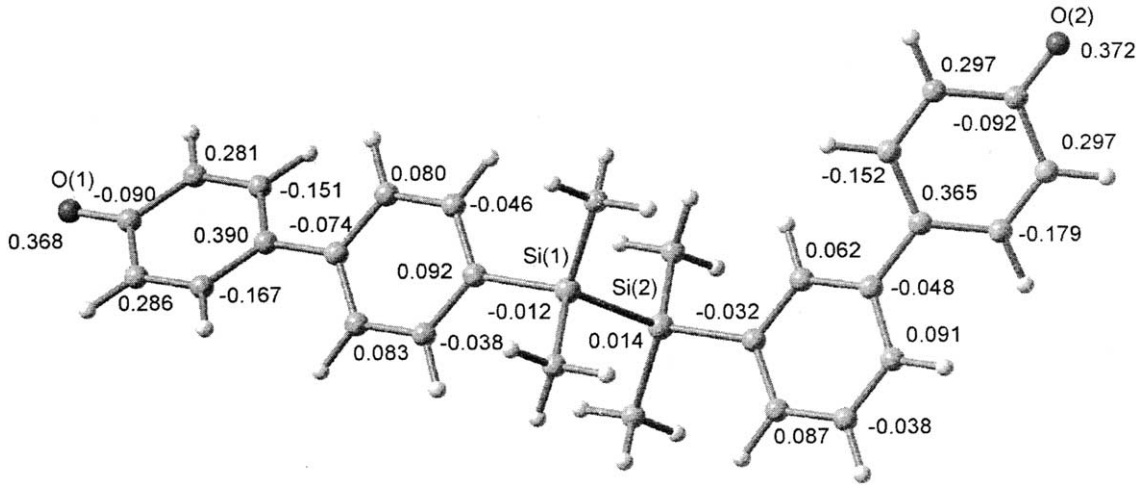

Fig. 3. Spin densities and optimized geometry of **8mp** derived from MO calculations at the UB3LYP/6-31+G(d) level.

tion of the aqueous layer with ether or chloroform, drying the combined organic layer and extracts with anhydrous magnesium sulfate, and evaporation of the solvent. Diethyl ether and THF were dried over sodium–potassium alloy and MTHF was dried over sodium. They were distilled just before use. (4-Bromo-2,6-di-*tert*-butylphenoxy)trimethylsilane was prepared as reported in the literature [9]. 3,5-Di-*tert*-butyl-4-trimethylsiloxyphenyllithium and 3- and 4-(3,5-di-*tert*-butyl-4-trimethylsiloxyphenyl)phenyllithium were prepared by treating the corresponding aryl bromides with one equivalent of *n*-butyllithium. For oxidation of precursors leading to phenoxyl radicals, freshly prepared PbO_2 must be used [10]. Commercially available PbO_2 did not react with the precursors at all. ESR spectra were measured on Brucker ESP 300E, JEOL JES-RE1X and JFS-FE1X spectrometers, using MTHF as the solvent (10 mM), at the temperature range of 6–80 K and room temperature (r.t.).

4.2. Preparation of *1a* and *1b*

To a solution of 3,5-di-*tert*-butyl-4-trimethylsiloxyphenyllithium in diethyl ether was added 0.42 g (2.80 mmol) of 1,2-dichlorotetramethyldisilane at −78 °C and the resulting mixture was stirred at r.t. for 2 h. After work up of the reaction mixture, the crude product was recrystallized from acetone/chloroform (10/1) to give 1.40 g (93% yield) of **1b** as the colorless solids: m.p. 186.5–188.0 °C; MS *m/z* 670 [M^+]; ^{1}H-

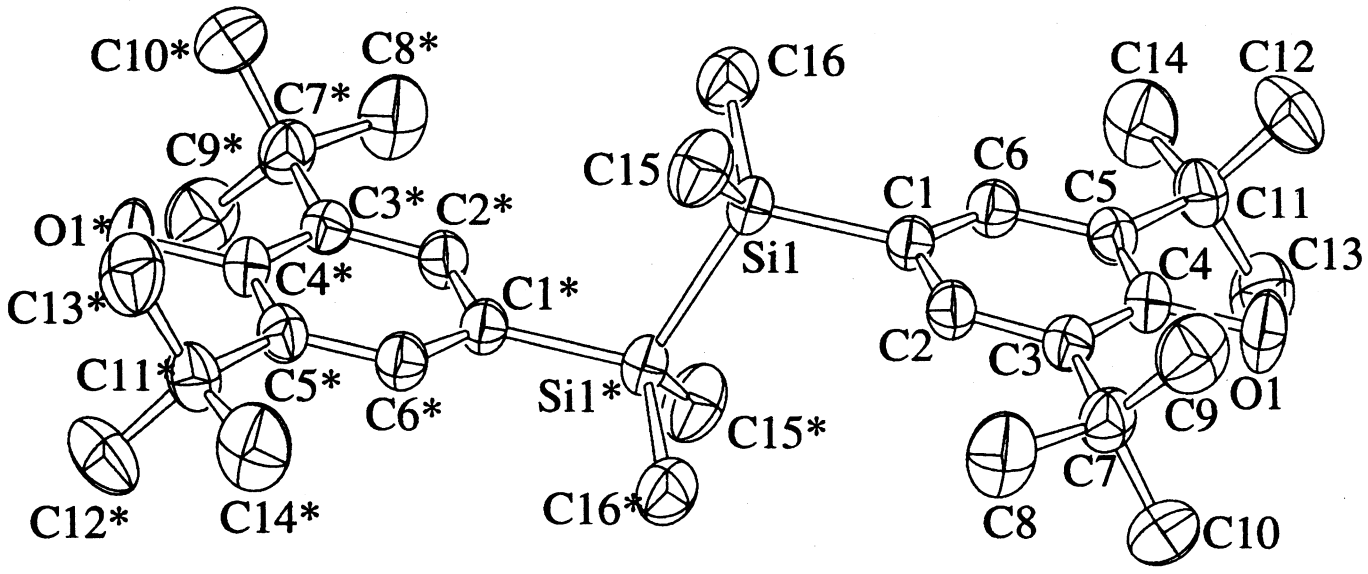

Fig. 4. ORTEP drawing of compound **2b**. Protons are omitted for clarity. Thermal ellipsoids are drawn at 50% probability. Selected bond distances (Å) and bond angles (°): Si1–Si1*, 2.345(2); Si1–C1, 1.883(3); C1–C2, 1.393(4); C2–C3, 1.391(4); C3–C4, 1.410(4); C4–C5, 1.404(4); C5–C6, 1.394(4); C6–C1, 1.392(4); O1–C4, 1.385(3); Si1*–Si1–C1, 109.9(1); Si1–C1–C2, 119.3(2); Si1–C1–C6, 123.6(2); C6–C1–C2, 117.1(2); C1–C2–C3, 123.7(3); C2–C3–C4, 116.5(3); O1–C4–C3, 118.1(3); O1–C4–C5, 119.4(3); C3–C4–C5, 122.5(2); C4–C5–C6, 117.2(3); C5–C6.

NMR ($CDCl_3$) δ 0.30 (s, 12H), 0.38 (s, 18H), 1.35 (s, 36H), 7.27 (s, 4H); ^{13}C-NMR ($CDCl_3$ at 25 °C) δ −3.12, 3.93, 31.28, 31.37, 35.08, 129.41, 131.50, 131.56, 139.66, 153.68; ^{13}C-NMR ($CDCl_3$ at 45 °C) δ −3.13, 3.89, 31.44, 35.14, 129.47, 131.56, 139.81, 153.73; ^{29}Si-NMR ($CDCl_3$) δ −21.95, 13.42. Anal. Calc. for $C_{38}H_{70}O_2Si_4$: C, 67.98; H, 10.51. Found: C, 67.87; H, 10.61%.

Compound **1a** was obtained similar to above, using dichlorodimethylsilane instead of dichlorotetramethyldisilane as the starting substance: 93% yield (after recrystallization from acetone–chloroform (10/1)): m.p. 174–176 °C; MS *m/z* 612 [M^+]; ^{1}H-NMR ($CDCl_3$) δ 0.41 (s, 18H), 0.50 (s, 6H), 1.37 (s, 36H), 7.38 (s, 4H); ^{13}C-NMR ($CDCl_3$) δ −1.76, 3.96, 31.25, 31.29, 35.12, 129.17, 131.87, 139.64, 154.11; ^{29}Si-NMR ($CDCl_3$) δ −10.47, 11.93. Anal. Calc. for $C_{36}H_{64}O_2Si_3$: C, 70.52; H, 10.52. Found: C, 70.39; H, 10.53%.

4.3. Preparation of *2a* and *2b*

Methyllithium (3.64 ml, 4.15 mmol) in diethyl ether (1.14 M) was added to a solution of **1b** (1.27 g, 1.89 mmol) in 40 ml of THF at −30 °C. The mixture was stirred over night at r.t. After work-up of the mixture, the crude product was recrystallized from hexane to give 0.56 g (57% yield) of **2b** as the colorless solids: m.p. 160.5–164.0 °C; MS *m/z* 526 [M^+]; ^{1}H-NMR ($CDCl_3$) δ 0.31 (s, 12H), 1.38 (s, 36H), 5.18 (s, 2H, OH), 7.19 (s, 4H); ^{13}C-NMR ($CDCl_3$) δ −2.94, 30.36, 34.29, 128.37, 130.73, 134.87, 154.42; ^{29}Si-NMR ($CDCl_3$) δ −21.67; IR 3630.3 cm^{-1} (O–H). Anal. Calc. for $C_{32}H_{54}O_2Si_2$: C, 72.94; H, 10.33. Found: C, 72.85; H, 10.39%.

Compound **2a** was obtained from **1a** in a similar fashion to above: 55% yield (after recrystallization from hexane): m.p. 189–191 °C; MS *m/z* 468 [M^+]; ^{1}H-NMR ($CDCl_3$) δ 0.50 (s, 6H), 1.42 (s, 36H), 5.26 (s, 2H, OH), 7.35 (s, 4H); ^{13}C-NMR ($CDCl_3$) δ −1.75, 30.31, 34.34, 128.07, 130.97, 134.89, 154.80; ^{29}Si-NMR ($CDCl_3$) δ −8.73; IR 3635.6, 3619.2 cm^{-1} (O–H). Anal. Calc. for $C_{30}H_{48}O_2Si$: C, 76.86; H, 10.32. Found: C, 76.76; H, 10.27%.

4.4. Oxidation of *2a* and *2b*

PbO_2 (0.26 g, 1.09 mmol) was added to a solution of **2b** (0.05 g, 0.09 mmol) in 9.5 ml of MTHF at r.t. The mixture was stirred for 30 min. After Pb salts were filtered and the solvent was evaporated, the residue was subjected to silica gel chromatography, eluting with hexane–ethyl acetate (10/1) to give 0.03 g (80% yield) of tetra-*tert*-butyldiphenoquinone: m.p. 210–212 °C; MS *m/z* 408 [M^+]; ^{1}H-NMR ($CDCl_3$) δ 1.35 (s, 36H), 7.69 (s, 4H); ^{13}C-NMR ($CDCl_3$) δ 29.57, 36.01, 125.99, 136.11, 150.42, 186.46; IR 1601.8 cm^{-1} (C=O). Anal. Calc. for $C_{28}H_{40}O_2$: C, 82.30; H, 9.87. Found: C, 82.32; H, 9.92%.

Oxidation of **2a**, similar to above gave diphenoquinone in 98% yield.

4.5. Preparation of *4pp*

1,2-Dichlorotetramethyldisilane (0.76 g, 2.80 mmol) was added to a solution of 4-(3,5-di-*tert*-butyl-4-trimethylsiloxyphenyl)phenyllithium in diethyl ether at −78 °C and the resulting mixture was stirred at r.t. for 2 h. After work-up of the reaction mixture, the crude product was recrystallized from hexane to give 1.78 g (56% yield) of **4pp** as the colorless solids: m.p. 179.0–181.5 °C; MS *m/z* 822 [M^+]; ^{1}H-NMR ($CDCl_3$) δ 0.36 (s, 12H), 0.42 (s, 18H), 1.44 (s, 36H), 7.44 (d, 4H, J = 7.85 Hz), 7.48 (s, 4H), 7.51 (d, 4H, J = 7.85 Hz); ^{13}C-NMR ($CDCl_3$) δ −3.70, 3.96, 31.31, 35.29, 124.55, 126.18, 132.78, 134.29, 136.69, 141.02, 141.83, 152.96; ^{29}Si-NMR ($CDCl_3$) δ −22.02, 13.99. Anal. Calc. for $C_{50}H_{78}O_2Si_4$: C, 72.92; H, 9.55. Found: C, 72.67; H, 9.56%.

4.6. Preparation of *4mp*

1,2-Dichlorotetramethyldisilane (0.60 g, 3.20 mmol) was added to a solution of 3-(3,5-di-*tert*-butyl-4-trimethylsiloxyphenyl)phenyllithium in diethyl ether at −78 °C and the resulting mixture was stirred at r.t. for 2 h, then again cooled down to −78 °C. To this was added 4-(3,5-di-*tert*-butyl-4-trimethylsiloxyphenyl)phenyllithium and the resulting mixture was stirred at r.t. for 2 h. After work-up of the reaction mixture, the crude product was subjected to silica gel chromatography, eluting with hexane–ethyl acetate (50/1) to give 1.51 g (72% yield) of **4mp** as the colorless solids: m.p. 135.1–136.5°C; MS *m/z* 822 [M^+]; ^{1}H-NMR ($CDCl_3$) δ 0.37 (s, 6H), 0.38 (s, 6H), 0.43 (s, 18H), 1.43 (s, 18H), 1.44, (s, 18H), 7.35 (d, 1H, J = 7.25 Hz), 7.36 (t, 1H, J = 7.25 Hz), 7.44 (d, 2H, J = 7.62 Hz), 7.45 (s, 2H), 7.46 (s, 2H), 7.50 (d, 1H, J = 7.25 Hz), 7.50 (d, 2H, J = 7.62 Hz), 7.64 (s, 1H); ^{13}C-NMR ($CDCl_3$) δ −3.74, −3.62, 3.96, 4.00, 31.23, 31.27, 35.24, 35.27, 124.55, 124.68, 126.18, 127.21, 127.96, 132.03, 132.47, 132.74, 133.26, 134.24, 135.27, 136.60, 139.38, 140.94, 141.05, 141.83, 152.80, 152.93; ^{29}Si-NMR ($CDCl_3$) δ −21.97, −21.52, 13.87, 13.96.

4.7. Preparation of *5pp* and *5mp*

Potassium carbonate (0.18 g) in 1 ml of water was added to a solution of **4pp** (0.10 g, 0.12 mmol) in 5 ml of THF. The mixture was stirred over night at r.t. After work-up of the resulting mixture, the crude product was recrystallized from hexane to give 0.08 g (90% yield) of **5pp** as the colorless solids: m.p. 242–244 °C; MS *m/z*

678 [M^+]; ^{1}H-NMR ($CDCl_3$) δ 0.36 (s, 12H), 1.48 (s, 36H), 5.25 (s, 2H OH), 7.39 (s, 4H), 7.44 (d, 4H, $J = 7.85$ Hz), 7.49 (d, 4H, $J = 7.85$ Hz); ^{13}C-NMR ($CDCl_3$) δ −3.72, 30.34, 34.47, 123.95, 126.27, 132.39, 134.28, 136.15, 136.60, 142.16, 153.53; ^{29}Si-NMR ($CDCl_3$) δ −21.99; IR 3637.5 cm^{-1} (O–H). Anal. Calc. for $C_{44}H_{62}O_2Si_2$: C, 77.81; H, 9.20. Found: C, 77.86; H, 9.29%

Compound **5mp** was prepared in a similar fashion to above as the colorless solids: 90% yield (after purification by silica gel column chromatography): m.p. 118.5–120.0 °C; MS *m/z* 678 [M^+]; ^{1}H-NMR ($CDCl_3$) δ 0.36 (s, 6H), 0.37 (s, 6H), 1.46 (s, 18H), 1.47, (s, 18H), 5.24 (s, 1H, OH), 5.25(s, 1H, OH), 7.34 (t, 1H, $J = 6.77$ Hz), 7.35 (d, 1H, $J = 6.77$ Hz), 7.35 (s, 2H), 7.37 (s, 2H) 7.43 (d, 2H, $J = 8.09$ Hz), 7.47 (d, 2H, $J = 8.09$ Hz), 7.48 (d, 1H, $J = 6.77$ Hz), 7.60 (s, 1H); ^{13}C-NMR ($CDCl_3$) δ −3.75, −3.62, 30.31, 30.34, 34.43, 34.46, 123.96, 124.10, 126.28, 127.28, 127.96, 131.98, 132.37, 132.60, 132.92, 134.24 (two carbons), 136.13, 136.52, 139.44, 141.43, 142.19, 153.40, 153.53; ^{29}Si-NMR ($CDCl_3$) δ −21.92, −21.49; IR 3640.4 cm^{-1} (O–H). Anal. Calc. for $C_{44}H_{62}O_2Si_2$: C, 77.81; H, 9.20. Found: C, 77.86; H, 9.26%.

4.8. Preparation of *6pp* and *6mp*

Phenoxyl radicals **6pp** and **6mp** were obtained from **5pp** and **5mp**, respectively, by oxidation with PbO_2 in large excess, similar to attempted preparation of **3a**,**b** described above. After filtration of PbO_2, the filtrate was directly subjected to the ESR measurements. ESR data: $g = 2.0051$ for **6pp** and $g = 2.0055$ for **6mp**.

4.9. MO calculational method

MO calculations were carried out on the density functional theory (DFT) at GAUSSIAN-98 program [11]. For calculations of the singlet state of phenoxyl radical **8mp**, attempted geometry optimization at the level of UB3LYP/6-31G failed. In these calculations, we obtained geometries with unusual spin densities or did not succeed to find out geometries with energy minimum. Therefore, we carried out the singlet state energy calculations using the optimized geometries of the triplet state molecule of **8mp**. Calculations using a keyword of Guess = Mix led to successful results with $\langle S \rangle^2 = 1$. Other calculations on **7mp** and the triplet molecule of **8mp** were readily performed as described in the section of results and discussion.

4.10. X-ray crystallographic analysis of *2b*

The crystal date and refinement parameters are summarized in Table 1. The structure was solved by SIR-92 direct methods [12] and expanded using DIRDIF-94 Fourier techniques [13]. The non-hydrogen atoms were refined anisotropically. Neutral atom scattering factors were taken from Cromer and Waber [14]. Anomalous dispersion effects were included in F_{calc} [15]; the values for $\Delta f'$ and $\Delta f''$ were those of Creagh and McAuley [16]. The values for the mass attenuation coefficients are those of Creagh and Hubbel [17]. All calculations were performed using the TEXSAN [18] crystallographic software package of Molecular Structure Corporation.

Table 1
Crystal data, experimental conditions, and summary of structural refinement for **2b**

Compound	**2b**
Molecular formula	$C_{32}H_{54}O_2Si_2$
Molecular weight	526.95
Crystal system	Triclinic
Space group	$P\bar{1}$ (no. 2)
Unit cell dimensions	
a (Å)	9.726(2)
b (Å)	14.402(3)
c (Å)	6.320(1)
α (°)	93.74(2)
β (°)	102.17(2)
γ (°)	104.29(2)
V (Å^3)	832.2(3)
Z	1
D_{calc} (g cm^{-3})	1.051
F_{000}	290.00
Crystal size (mm^3)	0.3 × 0.3 × 0.1
Crystal color	Colorless
μ (cm^{-1})	1.30
Diffractometer	Rigaku AFC-7R
Temperature (K)	296
Wavelength (Å)	0.71069 (Mo Kα)
Monochromator	Graphite crystal
Scan type	ω–2θ
Scan speed (deg min^{-1})	8
Scan width (°)	$6 \leq 2\theta \leq 55$
No. of unique reflns	3819
No. of observed reflections	2004($I \geq 3\sigma(I)$)
Reflections/parameter ratio	12.29
Corrections	None
R	0.046
R_w [a]	0.046

[a] Weighting scheme is $(\sigma(F_o)^2 + 0.0004|F_o|^2)^{-1}$.

5. Supplementary material

Crystallographic data for the structural analysis have been deposited with the Cambridge Crystallographic Data Centre, CCDC no. 212529 for compound **2b**. Copies of this information may be obtained free of charge from The Director, CCDC, 12 Union Road, Cambridge CB2 1EZ, UK (Fax: +44-1223-336033; e-mail: deposit@ccdc.cam.ac.uk or www: http://www.ccdc.cam.ac.uk).

Acknowledgements

This work was supported in part by NEDO (project no. 01A26005a). We thank Sankyo Kasei Co. Ltd. for financial support, and Shin-Etsu Chemical Co. Ltd. for the gift of chlorosilanes. We also thank Prof. N. Koga (Kyushu University) for the valuable suggestions.

References

[1] (a) J. Ohshita, A. Kunai, Acta Polym. 49 (1998) 379;
(b) M. Ishikawa, J. Ohshita, Silicon and germanium containing conductive polymers, in: H.S. Nalwa (Ed.), Handbook of Organic Conductive Molecules and Polymers, Ch. 15, vol. 2, Wiley, New York, 1997;
(c) M. Zeldin, H.K.J. Wynne, R. Allcock (Eds.), Inorganic and Organometallic Polymers, ACS Symposium Series 368, American Chemical Society, Washington, DC, 1988.;
(d) J.M. Zeigler, F.W.G. Fearon (Eds.), Silicon-Based Polymer Science, Advances in Chemistry Series 224, American Chemical Society, Washington, DC, 1990.

[2] (a) For reviews, see H. Iwamura, N. Koga, Acc. Chem. Res. 26 (1993) 346;
(b) A. Rajca, Chem. Rev. 94 (1994) 871;
(c) P.M. Lahti, Magnetic Properties of Organic Materials, Marcel Dekker, New York, 1999;
(d) K. Itoh, M. Kinoshita, Molecular Magnetism: New Magnetic Materials, Kodansha and Gordon & Breach, Tokyo, 2000.

[3] (a) For recent works, see L. Ducasse, A. Fritsch, Chem. Phys. Lett. 286 (1998) 183;
(b) H. Nishide, R. Doi, K. Oyaizu, E. Tsuchida, J. Org. Chem. 66 (2001) 1680;
(c) A. Rajca, S. Rajca, J. Wougsriratanakul, J. Am. Chem. Soc. 121 (1999) 6308;
(d) M. Miyasaka, T. Yamazaki, E. Tsuchida, H. Nishide, Macromolecules 33 (2000) 8211;
(e) S.V. Chapyshev, R. Walton, J.A. Sanborn, P.M. Lahti, J. Am. Chem. Soc. 122 (2000) 1580;
(f) V.M. Domingo, X. Burdous, E. Brillas, J. Carilla, J. Rius, X. Torrelles, L. Juliá, J. Org. Chem. 65 (2000) 6847;
(g) V.M. Domingo, C. Alemán, E. Brillas, L. Juliá, J. Org. Chem. 66 (2001) 4058;
(h) P.M. lahti, Y. Liao, M. Julier, F. Palacio, Syn. Met. 122 (2001) 485;
(i) H. Nishide, T. Maeda, K. Oyaizu, E. Tsuchida, J. Org. Chem. 64 (1999) 7129;
(j) H. Nishide, T. Ozawa, M. Miyasaka, E. Tsuchida, J. Am. Chem. Soc. 123 (2001) 5942;
(k) T. Kaneko, T. Makino, H. Miyaji, M. Teraguchi, T. Aoki, M. Miyasaka, H. Nishide, J. Am. Chem. Soc. 125 (2003) 3554.

[4] T. Doi, A. Ichimura, N. Koga, H. Iwamura, J. Am. Chem. Soc. 115 (1993) 8928.

[5] J. Ohshita, T. Iida, N. Ohta, K. Komaguchi, M. Shiotani, A. Kunai, Org. Lett. 4 (2002) 403.

[6] T. Iida, J. Ohshita, T. Uemura, H. Fukuoka, N. Ohta, K. Komaguchi, Y. Itagaki, M, Shiotani, S. Yamanaka, A. Kunai, Silicon Chemistry, in press.

[7] Synthesis of compounds **1a** and **2a** have been reported, previously, but the yields were rather low. S.D. Pastor, E.T. Hessell, J. Organomet. Chem. 376 (1989) 21.

[8] H. Nishide, T. Kaneko, T. Nii, K. Katoh, E. Tsuchida, P.M. Lahti, J. Am. Chem. Soc. 118 (1996) 9695.

[9] W. Harrer, H. Kurreck, J. Reusch, W. Girke, Tetrahedron 31 (1975) 625.

[10] Y. Morita, T. Ohba, N. Haneda, S. Maki, J. Kawai, K. Hatanaka, K. Sato, D. Shiomi, T. Takui, K. Nakasuji, J. Am. Chem. Soc. 19 (2000) 4825.

[11] GAUSSIAN-98, revision A.9, Gaussian Inc., Pittsburgh, PA.

[12] A. Altomare, M.C. Burla, M. Camalli, M. Cascarano, C.C. Giacovazzo, A. Guagliardi, G. Polidori, J. Appl. Crystallogr. 27 (1994) 1045.

[13] P.T. Beurskens, G. Admiraal, G Beurskens, W.P. Bosman, R. de Gelder, R. Israel, J.M.N. Smits, The DIRDIF-94 program system, Technical Report of the Crystallography Laboratory, University of Nijmegen, The Netherlands, 1994.

[14] D.T. Cromer, J.T. Waber, International Tables for X-ray Crystallography, Table 2.2A, vol. 4, Kynoch, Birmingham, UK, 1974.

[15] J.A. Ibers, W.C. Hamilton, Acta Crytallogr. 17 (1964) 781.

[16] D.C. Creagh, W.J. McAuley, in: A.J.C. Wilson (Ed.), International Tables for Crystallography, Table 4.2.4.8, vol. C, Kluwer, Boston, MA, 1992, pp. 219–222.

[17] D.C. Cregh, J.H. Hubbell, in: A.J.C. Wilson (Ed.), International Tables for Crystallography, Table 4.2.4.3, Kluwer, Boston, MA, 1992, pp. 200–206.

[18] TEXSAN, Crystal Structure Analysis Package, Molecular Structure Corporation, 1985 and 1992.